

Classification of Pneumonia from Chest X-ray Image using Machine Learning Models

D. Sreenivasa Rao¹, Dr. S. Anu H Nair², Dr. Thota Venkat Narayana Rao³, Dr. K. P. Sanal Kumar^{4*}

Submitted: 06/06/2022

Accepted: 10/09/2022

Abstract: Chest X-ray images are extremely difficult to interpret due to the fact that they are produced using a projection imaging modality. This is largely owing to the fact that anatomical structure and disease are closely intertwined. A large number of chest X-rays helps radiologists develop their knowledge and diagnostic abilities after they have mastered the principles of chest X-ray analysis. Droplets fill the lungs and make breathing difficult as a result of pericardial effusion caused by pneumonia. Pneumonia can be treated more effectively and with a higher chance of survival if caught early. Chest X-ray imaging is the most routinely used diagnostic technique for pneumonia. Examining chest X-rays, on the other hand, is a tough task with a high degree of subjectivity. In this study, we employed chest X-ray pictures to develop a computer-aided specialised diagnostic system capable of identifying pneumonia. Researchers have seen how machine learning algorithms can be used to tell if a chest X-ray shows signs of pneumonia. The most important thing about this study's conclusion is that it sorts out the different types of pneumonia. The combined Scale Invariant Fourier Transform (SIFT) and Local Binary Pattern (LBP) features are extracted from each training image and fed into machine learning models such as the Random Forest (RF), Artificial Neural Network (ANN) and Decision Tree (DT) model. After that, the classification model was created and tested on a set of test images. With an accuracy of 91.29%, RF was able to correctly classify all of the patients who had been diagnosed with pneumonia. Based on these results, we can say that the proposed method described in this research paper may help doctors figure out what's wrong with people with typical pneumonia.

Keywords: Pneumonia, Machine Learning, Classification, Traditional Learning, and X-ray images.

1 Introduction

A bacterial, viral, or fungal infection of the lungs can result in pneumonia. It produces pericardial effusion, a condition in which the lung becomes engorged with fluid, as well as pain in the airways. Among children under the age of five, it is responsible for more than 15% of fatalities. Many people in undeveloped and underdeveloped countries

suffer from pneumococcal disease because of an inadequate health resources and population expansion. A person's life can be saved if the disease is diagnosed and treated early. In order to diagnose lung disease, a variety of imaging techniques are utilised, including X-rays, CT scans, MRIs, and radiography. X-ray imaging is a low-cost, non-invasive method of examining the lungs.



A) Healthy Lung



B) Pneumonic Lung

Figure 1: Example X-ray image of a) Healthy Lung and b) Pneumonic Lung

Chemotherapy is a noninvasive diagnostic imaging procedure that makes it possible to see images of the chest and the organs inside it. There are a lot of people who have it. With an X-ray machine, a picture of the chest is taken and saved on film or in a computer system so that the chest condition of the patient can be found quickly. X-rays of the

chest are also called chest radiographs (CT), chest roentgenograms, or CXRs, among other names. Depending on how thick it is, each organ in the chest cavity keeps different amounts of radiation, which makes shadows on the motion picture. Images from a chest X-ray have a lot of contrast, so the only way to tell the different parts of the chest apart is by how bright or hazy the image is. As an example, the bones and vertebral column of the chest wall absorb more radiation than other parts of the body. Because of this, they appear whiter on film.

Doctors order chest X-rays for many reasons, particularly cancer screening. This radiological exam can evaluate many health problems. Chest X-rays can reveal pneumonia, an enlarged heart, congestive heart failure, lung mass, and pleural effusion. As projection images, chest X-rays are difficult to interpret. Morphological structure and disease are tightly linked. Differentiating diseased from healthy structures, like

¹Research Scholar, Department of Computer Science and Engineering, Annamalai University, Chidambaram, India. (Assistant Professor, Department of CSE, Sreenidhi Institute of Science & Technology, Telangana).

Email: devavarapusreenivasarao18@gmail.com

²Assistant Professor, Department of CSE, Annamalai University, Chidambaram, India (Deputed to WPT Chennai). Email: anu_jul@yahoo.co.in

³Professor, Department of CSE and HOD-CSE(IoT), Sreenidhi Institute of Science & Technology, Yamnampet, Ghatkesar R R Dist. Telangana. Email: venkatmarayanaraot@sreenidhi.edu.in

⁴Assistant Professor, P.G Department of Computer Science, R. V. Government Arts College, Chengalpattu, India. Email: sanalprabha@yahoo.co.in

*Corresponding Author

lung infiltration and blood vessel architecture, can be difficult. After mastering chest X-ray analysis, a significant number of X-rays helps radiologists enhance their knowledge and diagnostic abilities. Radiologists memorise a healthy patient's chest X-ray to compare to new patients'.

More and more people are falling victim to pneumonia, especially children. This is due to a combination of health conditions such as overcrowding, poor hygiene and malnourishment and a lack of accessible medical care, which are all common in developing and undeveloped countries. Pneumonia must be detected early if it is to be properly cured. Radiologists sometimes disagree on the interpretation of X-ray scans, which is why X-ray examination is the most prevalent method of diagnosis. Consequently, an automated disease diagnosis system (ADDS) capable of generalising is needed to accurately detect the condition. The use of ensemble learning in the classification of pneumonia patients has not been studied to the best of our knowledge, according to the literature review. Ensemble learning was used in this work because it includes the discriminatory features from all the base learners, allowing it to make better predictions.

Contribution

By combining two feature extraction methods is used to classify the Lungs X-ray data set. The combined SIFT and LBP feature extraction algorithm is used to extract features. There are three different classification methods that use feature vectors produced from SIFT and LBP feature extraction algorithms as inputs. Anaconda distributions' libraries are used in the tests, which are run in Python and can be run in Python environments. The SIFT and LBP feature extraction algorithms, as well as the RF, ANN, and DT classification algorithms, are all implemented in the Scikit-Image library. Summary of the main contribution is as follows:

- Dataset Preparation (Splitting of train and test data).
- Image pre-processing labeling using Multi-label Classification.
- We have extracted feature using SIFT and LBP feature extraction algorithm.
- We have trained the dataset using machine learning algorithms like ANN, RF, and DT.
- We have recognized Chest X-ray image using machine learning algorithms.

Organization of paper

The remaining sections of this document are as follows: The works that are important to this study are discussed in Section 2. Detailed descriptions of the proposed feature preprocessing and extraction algorithms are provided in Section 3, along with code examples. Section 4 explains the machine learning model in greater detail. Section 5 describes the discussion of experimental results. Section 6 summarizes the study's conclusions and the dataset that was utilised to support them.

2 Related Works

This section covers the basics of radiography, including how it's used in medical imaging and how it might help with diagnosis. Pattern recognition, an applied way to classifying segmented images, is also discussed in this section. In addition, this research article provides a full

Due to the subjectivity of this procedure, there are often large discrepancies in chest X-ray interpretations amongst radiologists.

Motivation

review of the background of relevant image processing and feature extraction approaches, such as those discussed in this work. Machine learning techniques for supervised and unsupervised learning are introduced, as well as the Support Vector Machine (SVM), which serves as a basis for machine learning and has been widely employed in this study's classification phase.

Pneumonia researchers are using real-time reverse transcription reaction (RT-PCR). In order to diagnose the disease in its earliest stages, diagnostic imaging such as CT scans and X-rays are needed. It is possible to detect symptoms in radiographic pictures, despite RT-modest PCR's sensitivity (60–70 percent) [11, 12]. By using CT scans, as well as RT-PCR screening, it is possible to diagnose COVID-19 pneumonia. Within the initial 0–2 days of the onset of symptoms, CT scans are commonly conducted [12]. CT scan results are frequently noticed several days after the onset of symptoms. X-rays of the lungs of patients who survived COVID-19 pneumonia revealed the most severe lung illness 10 days after the onset of symptoms [14]. Doctors advised patients to undergo physical examinations and chest CT scans in order to diagnose the onset of the pandemic in China because of reports that diagnostic kits in hospitals were lacking and that a high rate of false negative tests had been reported [7, 17-18]. A number of studies have shown that improvements were evident before the effects of COVID-19 were noticed [19].

One out of every three persons examined by Yoon and colleagues [20] had an unilateral granular impurity in the lower left lung. A stiffening of the lungs' fourth and fifth lobes was present in both patients who were also being treated for this condition. According to Zhao et al. [21], vascular dilatation and convergence were observed in a number of individuals with mixed GGOs during their study. There were lateral foci or numerous GGOs observed in 50% of individuals in another investigation [11]. Zu and colleagues discovered rounded lung illumination in 33% of chest CT images. The application of these techniques resulted in the development of an effective and reliable X-ray and CT scan imaging system.

Radiologists use chest X-rays or CT scans to distinguish between a patient with pneumonia and a healthy one. Infected patients have "Ground-glass opacity," which is the absence of white hazy patches in healthy individuals. SAR-CoV-2 and bacteria can cause severe pneumonia, but there is no test for COVID-19 and the RT-PCR method is expensive, time-consuming, inefficient, and labor-intensive [22-38]. A outcome of this is that researchers are increasingly turning to chest scanning techniques such as CT scans and X-rays as an alternate means of diagnosis. The fact that there are so few professionals (i.e. radiologists) who can interpret thousands of CT scans and CXR images only serves to exacerbate the situation. Models powered by artificial intelligence (AI) have shown high efficacy in helping medical experts classify and predict diseases [29-32].

3 Methodology of research work

This work covers numerous areas of the classification of chest X-ray images, including preprocessing, feature extraction, and classification models. This is in accordance with the purpose that we have established for ourselves. Figure 1 presents an illustration of the overall system architecture of the methodology that has been provided.

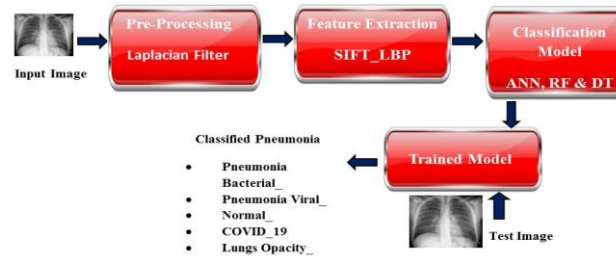


Figure 1: Overall Architecture of Proposed Methodology

We know that the edges of objects change in terms of brightness and contrast. The image is said to be sharp if this difference is noticeable. In this image, the viewer can clearly distinguish between the foreground and the

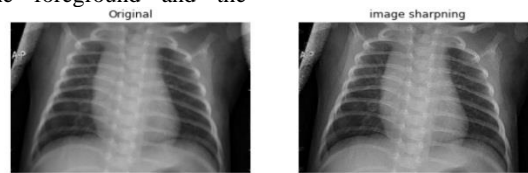


Figure 2: Preprocessed Image (a) Original Image (b) Image Sharpening

3.2 Combined Feature Extraction

Feature Extraction using SIFT feature

Local feature descriptors that are unaffected by changes in illumination, scaling, or rotation can be found and extracted using the Scale Invariant Feature Transform (SIFT). The author [15] was the first to come up with this algorithm. Improved and developed in recent years. SIFT has a number of advantages, including the following: images of natural features. They can be combined and used to generate useful information because they have good efficiency and speed, are invariant to uniform scaling and orientation, and are partially invariant to changes in illumination. 4 steps comprise the SIFT feature's detection stage:

The image $I(x, y)$ is first concatenated with Gaussian filters at various scales as the equation for this step:

$$L(x, y, \sigma) = G(x, y, \sigma) * I(x, y)$$

This is the convolution of image $I(x, y)$ with Gaussian filter $G(x, y, \sigma)$ at scale in the following equation. Equation 2.2 shows the differences between two Gaussian images at scales $k\sigma$ and σ as follows:

$$D(x, y, \sigma) = L(x, y, k\sigma) - L(x, y, \sigma)$$

3.1 Preprocessing

Image sharpening is a technique for improving the clarity of digital images. The edges of an image are better defined when it has been sharpened. The images that are drab are those that are pixelated at the edges. Edges and background are nearly indistinguishable. Contrary to popular belief, a sharper image is one in which the viewer can clearly make out the edges of objects.

background. The laplacian filter is used for sharpening the input image. The Figure 2 shows the original image and sharpening image.

The difference between these two scales is known as a DoG (Differences of Gaussians). Local maxima and minima of the DoG images are identified as keypoints, which can also be called Interest points, in this first stage of the analysis process. As depicted in the figure, each DoG image pixel is compared to its eight neighbouring pixels at the same scale. In addition, a predetermined number of points must be removed from the keypoint locations in order to improve their accuracy.

$$D(\hat{x}) = D + \frac{1}{2} \frac{\partial D^T}{\partial x} \hat{x}$$

An equation is used to precompute the gradient magnitude $m(x, y)$ and orientation $\theta(x, y)$ for orientation invariance.

$$m(x, y) = \sqrt{(L(x+1, y) - L(x-1, y))^2 + (L(x, y+1) - L(x, y-1))^2}$$

$$\theta(x, y) = \arctan\left(\frac{L(x, y+1) - L(x, y-1)}{L(x+1, y) - L(x-1, y)}\right)$$

An orientation histogram of 4×4 pixels is used to compute a feature descriptor for a keypoint orientation if it is selected. Using this method the STIP feature are extracted, which is shown in the figure 3.

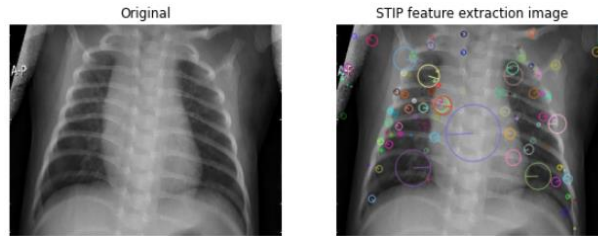


Figure 3: STIP feature extraction

Feature Extraction using LBP

Ojala and his colleagues came up with a simple and efficient way to find texture features. The Local Binary

Pattern (LBP) is one of them. This is how LBP did it: It used each data point as a threshold, then turned its 3 x 3 neighbourhood into an 8-bit binary code.

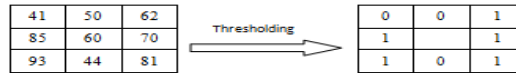


Figure 4: LBP Operator

Because of the binary code's predetermined order, texture direction information is reserved for pixels in between each byte. The binary pattern is known as uniform LBP and is denoted when it has at most two occurrences of 0 to 1 or 1 to 0.

The figure 4 explains the LBP operator. The figure 5 shows the visual of LBP image. The 1182 feature dimensions (bins) are extracted for each image.

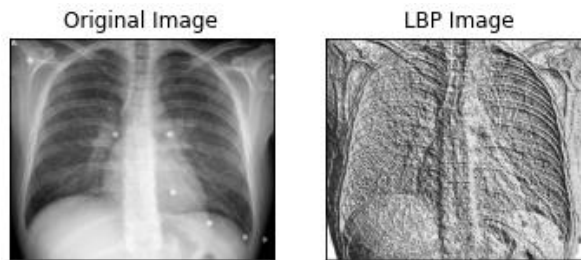


Figure 5: Visual of LBP Image

3.3 Classification Models

Artificial Neural Networks (ANN)

As a mathematical model of how information is processed in biological nerve systems, neural networks got their start

in this field. Progress in neural network complexity continues, but it is still far below that of the human mind.

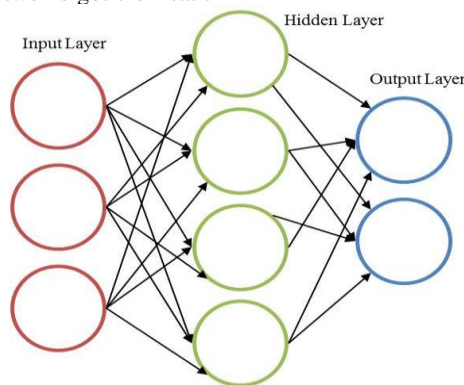


Figure 6: The structure of ANN

Understanding or estimating functions or making predictions in a pattern recognition context can be made much easier with neural networks. McCulloch and Pitts (1943) were the first to create a neural network, and Rosenblatt (1962) and Minsky and Seymour (1962) followed suit in the 1960s (1969). The introduction of the back-propagation learning algorithm (explained below) for training multi-layer perceptrons in the late 1980s ushered in the golden age of neural networks. In a certain network architecture, theoretical neurons are joined together to form

a neural network. Figure 6 depicts the construction of a neural network, where each circular node represents a synthetic neuron and each arrow denotes a communication between the each neurons.

Random Forest (RF)

It's possible to see a random forest as a collection of multiple decision trees. Using an averaging mechanism, the predictions from multiple decision trees are combined to produce a final result (majority voting). It improves the

model's ability to generalise to a larger population. Additional benefits include reduced overfitting and high variance in the model. Random forest algorithm's key steps are as follows:

- Select a random sample of n individuals (randomly choose n examples with replacement)
- Using the above sample, build a decision tree using the following:
 - Randomly select m features from all of the available features.
 - By using m features to break up the data, the tree can be constructed in accordance with the objective function (maximising the information gain).
 - As stated, repeat the above steps for the specified number of trees (k).

- Combine the predictions of different trees and come up with a final prediction based on the majority vote or average.

Decision Tree (DT)

When a decision tree is used to predict the dataset's class, the process begins at the root node. When the root attribute is compared to the record (actual dataset) attribute, it goes to the next node and follows the branch accordingly. The algorithm compares the variable with the other sub-nodes for the next node and then moves on to the next step. The procedure continues up to it reaches the tree's leaf node. The Figure 7 shows the Decision Tree Structure.

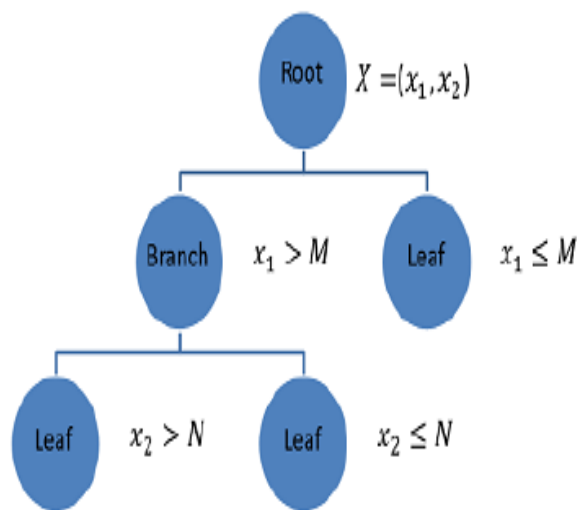


Figure 7: Decision Tree Structure

4 Experimental Analysis

Lungs X-Ray Dataset

Although more than 30 million people have been diagnosed with COVID-19, the number of CT scan images that can be accessed via the Internet is extremely limited and sparse. COVID-19 pneumonia, lung opacity, a normal CXR

image, pneumoniaviral and pneumoniabacterial CXR images, as illustrated in Figure 8, were received from the website: Keras (<https://www.kaggle.com/ta-wsifurrahman> or covid19-radiography-database) provides 1200 images from each category. The data set split for training and testing are 75% and 25%. The dataset's description is shown in the Table 1.

Table 1: Information about the Dataset

S. No.	Classes	Number of images
1.	Pneumonia-Bacterial	1200
2.	Pneumonia-Viral	1200
3.	Normal	1200
4.	COVID_19	1200
5.	Lungs Opacity	1200

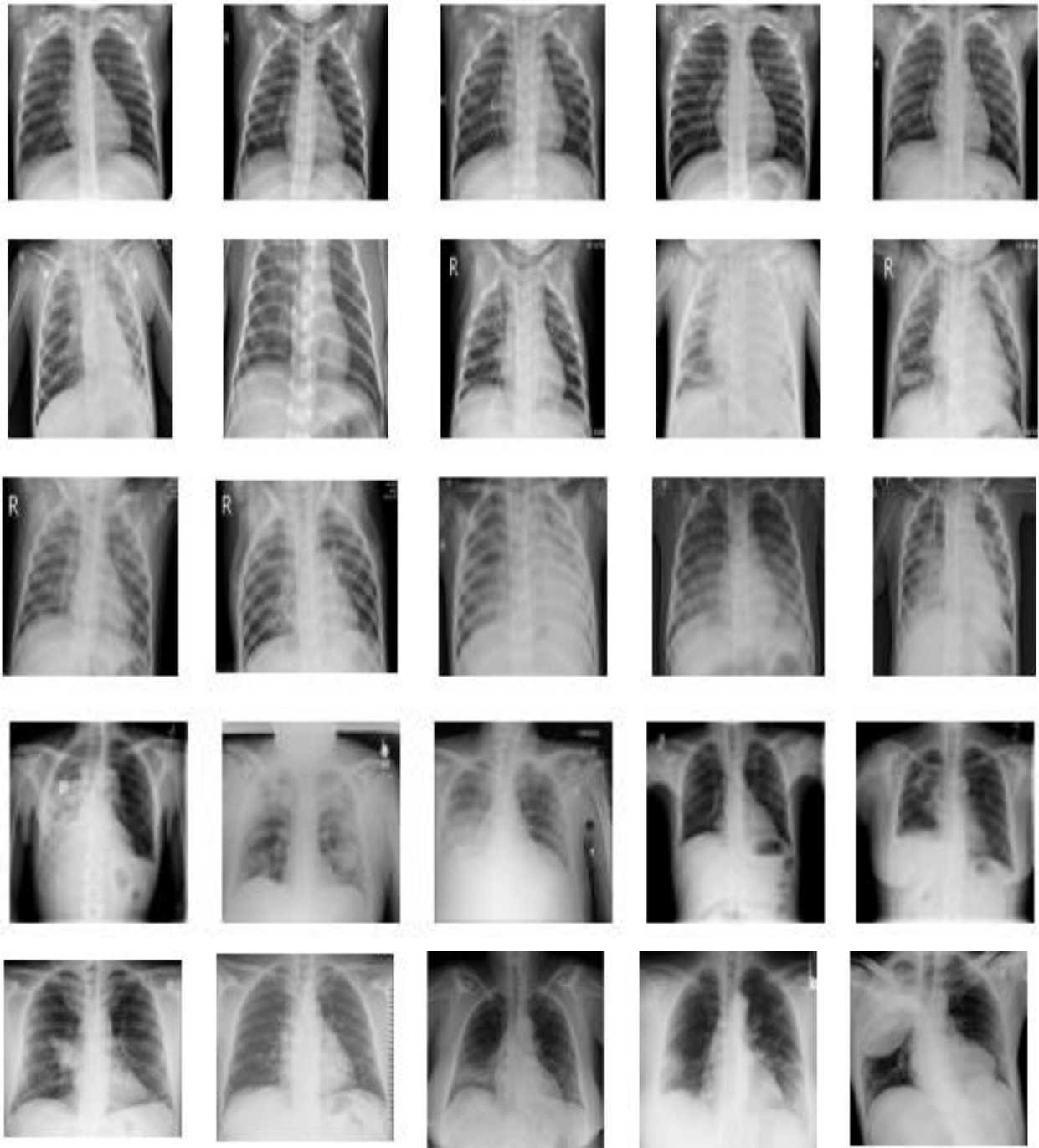


Figure 8: Sample datasets for Chest X-ray image

Performance Evaluation Metrics

The figure 6 shows the general confusion matrix table.

Predicted Class	Actual Class	
	True_Positive	False_Positive
	False_Negative	True_Negative

Figure 7: Table for Confusion Matrix

The overall accuracy reported for all approaches is calculated using the equation:

$$\text{Overall accuracy} = \frac{\text{Number of correctly classified videos}}{\text{Total number of videos in the test dataset}} \times 100\%$$

Similarly, the accuracy reported for a class is calculated using the equation:

$$\text{Class accuracy} = \frac{\text{Number of correctly classified class videos}}{\text{Total number of class videos in the test dataset}} \times 100\%$$

A confusion matrix is used to report all of the findings; in this matrix, each row stands for a different class label, and each column presents a different prediction. Other

metrics, such as precision, recall, and F1-scores, can be inferred from the confusion matrix by looking at the data. A relationship between the results that are considered to be truly positive and those that are considered to be truly negative can be used to express the level of precision. The following equation can be used to express it:

$$Recall = \frac{True\ Positives}{True\ Positive + True\ Negative} \times 100\%$$

$$F1 - Score = 2 \times \frac{Precision \times Recall}{Precision + Recall} \times 100\%$$

$$Precision = \frac{True\ Positives}{True\ Positive + True\ Positive} \times 100\%$$

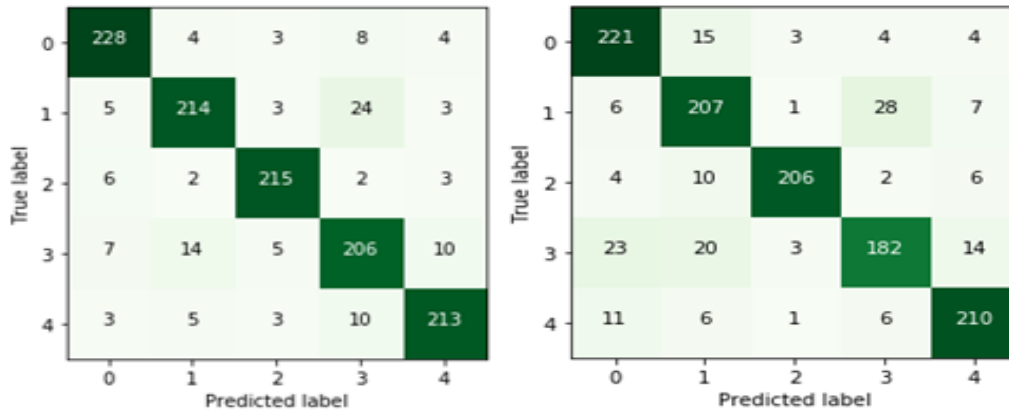


Figure 10: Confusion Matrix for RF and ANNC classifier

The Recall, Specificity, F-Score, Accuracy and Precision are the metrics used to evaluate the suggested classification models. The accuracy in classification tasks is the total number of true predictions made by the various machine

learning models. The Figure 10 and 11 enlighten the confusion matrix value for RF, ANN classifiers and KNN classifier respectively.

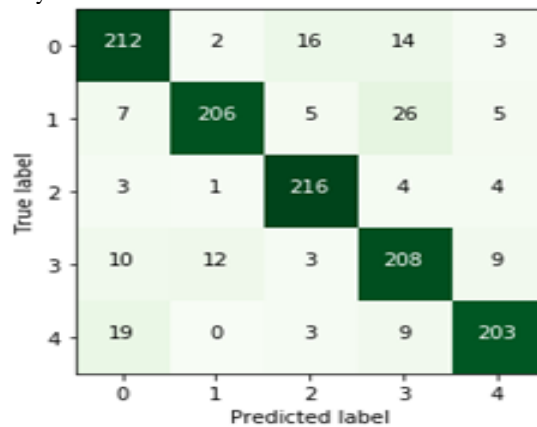


Figure 11: Confusion Matrix for DT Classifier

5 Discussion of Experimental Results

Each image's histogram was broken down into 64 individual bins and 1182 feature dimensions (bins) are extracted

for each image or LBP feature and the results of that process were presented in this section for your consideration.

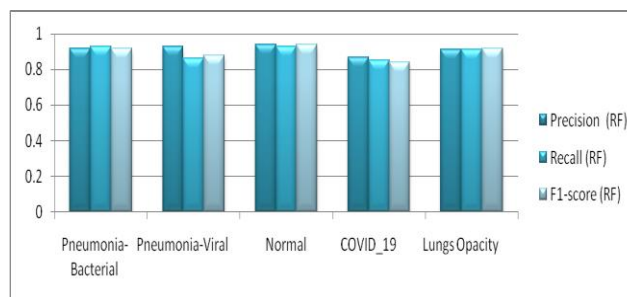


Figure 12: Class wise performance analysis for RF classifier

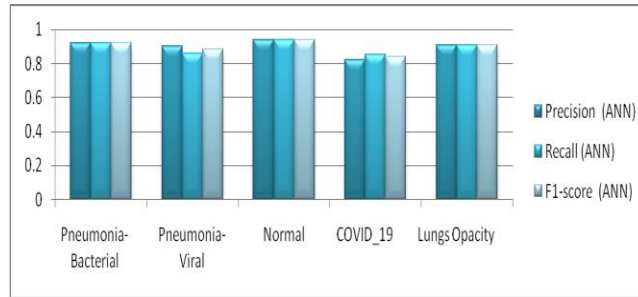


Figure 13: Class wise performance analysis for ANN classifier

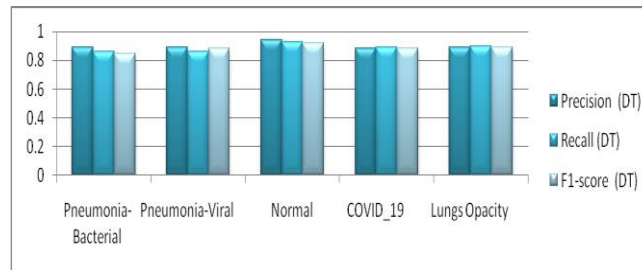


Figure 14: Class wise performance analysis for DT classifier

According to other algorithms, a STIP and LBP feature has the highest levels of accuracy. 91.29% accuracy was achieved using the RF algorithm. The ANN classifier had an accuracy of 88.41 percent, whereas the KNN classifier had an accuracy of 86.04 percent.

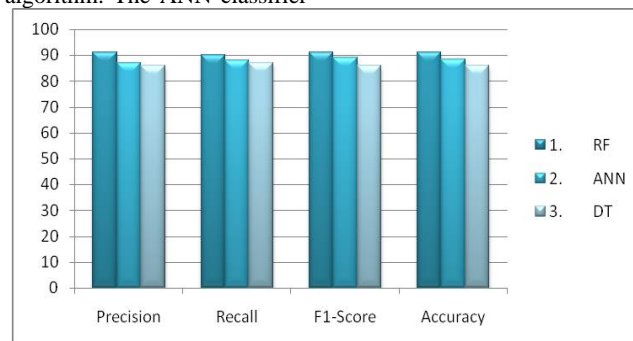


Figure 15: Performance Analysis of RF, ANN and DT models

The Figure 12, 13 and 14 visualize the class wise performance analysis for RF, ANN and DT classifier respectively. Table 2 summarises the results of an evaluation of machine learning models' performance (RF,

ANN and DT).The figure 15 explains the performance analysis of combined STIP and LBP feature with RF, ANN and DT machine learning models.

Table 2: Performance Analysis of Machine Learning Models (RF, ANN and DT)

S. No.	ML Models	Precision	Recall	F1-Score	Acc.
1.	RF	91	90	91	91.29
2.	ANN	87	88	89	88.41
3.	DT	86	87	86	86.04

6 Conclusion

The experiment conducted on Chest X-ray dataset using RF, ANN and DT classifiers shows that RF classifiers has outperformed the other methods specifically using SIFT and LBP feature. However the results obtained by ANN and DT classifiers were not satisfactory as the RF classifiers. But these parameters were chosen to ensure that the dimensions of each feature were consistent throughout

the different feature extractor models.RF classifiers have outperformed ANN and DT.

In Future, other pre-processing methods or contrast enhancement may be included in image quality upgrades. Prior to categorization, it may be beneficial to segment the lung image. The computational cost of the proposed ensemble is higher than that of prior CNN baselines since three CNN models are required to train it. Snapshot

ensembling may be used in the future to reduce computing requirements.

References

- [1] Zubair S. An Efficient Method to Predict Pneumonia from Chest X-Rays Using Deep Learning Approach. *The Importance Of Health Informatics In Public Health During A Pandemic*. 272 pp. 457 (2020)
- [2] WHO Pneumonia. World Health Organization. (2019), <https://www.who.int/news-room/factsheets/detail/pneumonia>
- [3] Neuman M., Lee E., Bixby S., Diperna S., Hellinger J., Markowitz R., et al. Variability in the interpretation of chest radiographs for the diagnosis of pneumonia in children. *Journal Of Hospital Medicine*. 7,294–298 (2012) <https://doi.org/10.1002/jhm.955> PMID: 22009855
- [4] Williams G., Macaskill P., Kerr M., Fitzgerald D., Isaacs D., Codarini M., et al. Variability and accuracy in interpretation of consolidation on chest radiography for diagnosing pneumonia in children under 5 years of age. *Pediatric Pulmonology*. 48, 1195–1200 (2013) <https://doi.org/10.1002/ppul.22806> PMID: 23997040
- [5] Kermany D., Zhang K. & Goldbaum M. Labeled Optical Coherence Tomography (OCT) and Chest XRay Images for Classification. (Mendeley, 2018)
- [6] Lal S., Rehman S., Shah J., Meraj T., Rauf H., Damas̃evičius R., et al. Adversarial Attack and Defence through Adversarial Training and Feature Fusion for Diabetic Retinopathy Recognition. *Sensors*. 21,3922 (2021) <https://doi.org/10.3390/s21113922> PMID: 34200216
- [7] Rauf H., Lali M., Khan M., Kadry S., Alolaiyan H., Razaq A., et al. Time series forecasting of COVID-19 transmission in Asia Pacific countries using deep neural networks. *Personal And Ubiquitous Computing*. pp. 1–18 (2021) <https://doi.org/10.1007/s00779-020-01494-0> PMID: 33456433
- [8] Deng J., Dong W., Socher R., Li L., Li K. & Fei-Fei, L. Imagenet: A large-scale hierarchical image database. *2009 IEEE Conference On Computer Vision And Pattern Recognition*. pp. 248–255 (2009)
- [9] Dalhoumi S., Dray G., Montmain J., Derosière, G. & Perrey S. An adaptive accuracy-weighted ensemble for inter-subjects classification in brain-computer interfacing. *2015 7th International IEEE/EMBS Conference On Neural Engineering (NER)*. pp. 126–129 (2015)
- [10] Albahli S., Rauf H., Algosaihi A. & Balas V. AI-driven deep CNN approach for multi-label pathology classification using chest X-Rays. *PeerJ Computer Science*. 7 pp. e495 (2021) <https://doi.org/10.7717/peerj-cs.495> PMID: 33977135
- [11] Rahman T., Chowdhury M., Khandakar A., Islam K., Islam K., Mahub Z., et al. Transfer learning with deep convolutional neural network (CNN) for pneumonia detection using chest X-ray. *Applied Sciences*. 10, 3233 (2020) <https://doi.org/10.3390/app10093233>
- [12] Liang G. & Zheng L. A transfer learning method with deep residual network for pediatric pneumoniadiagnosis. *Computer Methods And Programs In Biomedicine*. 187 pp. 104964 (2020) <https://doi.org/10.1016/j.cmpb.2019.06.023> PMID: 31262537
- [13] Ibrahim A., Ozsoz M., Serte S., Al-Turjman F. & Yakoi P. Pneumonia classification using deep learning from chest X-ray images during COVID-19. *Cognitive Computation*. pp. 1–13 (2021) <https://doi.org/10.1007/s12559-020-09787-5> PMID: 33425044
- [14] Rajpurkar P., Irvin J., Zhu K., Yang B., Mehta H., Duan T., et al. & Others CheXnet: Radiologist-level pneumonia detection on chest x-rays with deep learning. *ArXiv Preprint ArXiv:1711.05225*. (2017)
- [15] Ghebreyesus T, Lancet SS-T, 2020 U. Scientists are sprinting to outpace the novel coronavirus. *thelancet.com* 22. Mahase E. Covid-19: Russia approves vaccine without large scale testing or published results. *BMJ: British Med J (Online)*. 2020;13;370.
- [16] Beck BR, Shin B, Choi Y, Park S, Kang K. Predicting commercially available antiviral drugs that may act on the novel coronavirus (SARSCoV-2) through a drug-target interaction deep learning model. *Comput Struct Biotechnol J*. 2020.
- [17] Li Y, Zhang J, Wang N, Li H, Shi Y, Guo G, Liu K, Zeng H, Zou Q. Therapeutic drugs targeting 2019-nCoV main protease by high throughput screening. *BioRxiv*. 2020.
- [18] Vaishya R, Javid M, Khan IH, Haleem A. Artificial Intelligence (AI) applications for COVID-19 pandemic. *Diabetes & Metabolic Syndrome: Clin Res Rev*. 2020.
- [19] Zeng T, Zhang Y, Li Z, Liu X, Qiu B. Predictions of 2019-ncov transmission ending via comprehensive methods. *arXiv preprint arXiv: 2002.04945*. 2020.
- [20] Hu Z, Ge Q, Jin L, Xiong M. Artificial intelligence forecasting of covid-19 in china. *arXiv preprint arXiv: 2002.07112*. 2020.
- [21] LeCun Y, Bengio Y, Hinton G. Deep learning. *Nature*. 2015;521(7553):436–44.
- [22] Tan C, Sun F, Kong T, Zhang W, Yang C, Liu C. A survey on deep transfer learning. In *International Conference on Artificial Neural Networks 2018*. pp. 270–279. Springer Cham.
- [23] You Y, Zhang Z, Hsieh CJ, Demmel J, Keutzer K. Imagenet training in minutes. In *Proceedings of the 47th International Conference on Parallel Processing*. pp. 1–10. 2018.
- [24] Han X, Zhong Y, Cao L, Zhang L. Pre-trained alexnet architecture with pyramid pooling and supervision for high spatial resolution remote sensing image scene classification. *Remote Sens*. 2017;9(8):848.
- [25] Lippi G, Simundic AM, Plebani M. Potential preanalytical and analytical vulnerabilities in the laboratory diagnosis of coronavirus disease 2019 (COVID-19). *Clinical Chemistry and Laboratory Medicine (CCLM)*. 2020;1(ahead-of-print).
- [26] Chen N, Zhou M, Dong X, Qu J, Gong F, Han Y, Qiu Y, Wang J, Liu Y, Wei Y, Yu T. Epidemiological and clinical characteristics of 99

- cases of 2019 novel coronavirus pneumonia in Wuhan, China: a descriptive study. *The Lancet*. 2020;395(10223):507–13.
- [27] Ching T, Himmelstein DS, Beaulieu-Jones BK, Kalinin AA, Do BT, Way GP, Ferrero E, Agapow PM, Zietz M, Hofman MM, Xie W. Opportunities and obstacles for deep learning in biology and medicine. *J R Soc Interface*. 2018;15(141):20170387.
- [28] Kallianos K, Mongan J, Antani S, Henry T, Taylor A, Abuya J, Kohli M. How far have we come? Artificial intelligence for chest radiograph interpretation. *ClinRadiol*. 2019;1;74(5):338–45.
- [29] Wang F, Casalino LP, Khullar D. Deep learning in medicine—promise, progress, and challenges. *JAMA Intern Med*. 2019;179(3):293–4.
- [30] Wang W, Xu Y, Gao R, Lu R, Han K, Wu G, Tan W. Detection of SARS-CoV-2 in different types of clinical specimens. *Jama*. 2020; 12:323(18):1843–4.
- [31] Shan F, Gao Y, Wang J, Shi W, Shi N, Han M, Xue Z, Shi Y. Lung infection quantification of covid-19 in CT images with deep learning. arXiv preprint arXiv: 2003.04655. 2020.
- [32] Yang W, Yan F. Patients with RT-PCR-confirmed COVID-19 and normal chest CT. *Radiology*. 2020;295(2): E3-.
- [33] Apostolopoulos ID, Mpesiana TA. Covid-19: automatic detection from x-ray images utilizing transfer learning with convolutional neural networks. *PhysEngSci Med*. 2020;3:1.
- [34] Narin A, Kaya C, Pamuk Z. Automatic detection of coronavirus disease (covid-19) using x-ray images and deep convolutional neural networks. arXiv preprint arXiv: 2003.10849. 2020.
- [35] Wang L, Wong A. COVID-Net: A Tailored Deep Convolutional Neural Network Design for Detection of COVID-19 Cases from Chest X-Ray Images. arXiv preprint arXiv: 2003.09871. 2020
- [36] Albahli S., Rauf H., Arif M., Nafis M. &AlgoSaibi A. Identification of thoracic diseases by exploiting deepneural networks. *Neural Networks*. 5 pp. 6 (2021)
- [37] Chandra T. &Verma K. Pneumonia detection on chest X-Ray using machine learning paradigm. *Proceedings Of 3rd International Conference On Computer Vision And Image Processing*. pp. 21-33(2020)
- [38] Kuo K., Talley P., Huang C. & Cheng L. Predicting hospital-acquired pneumonia among schizophrenicpatients: a machine learning approach. *BMC Medical Informatics And Decision Making*. 19, 1–8 (2019)<https://doi.org/10.1186/s12911-019-0792-1> PMID: 30866913
- [39] Yue H., Yu Q., Liu C., Huang Y., Jiang Z., Shao C., et al. & Others Machine learning-based CT radiomics method for predicting hospital stay in patients with pneumonia associated with SARS-CoV-2 infection: a multicenter study. *Annals Of Translational Medicine*. 8 (2020) <https://doi.org/10.21037/atm-20-3026> PMID: 32793703
- [40] Sharma H., Jain J., Bansal P. & Gupta S. Feature extraction and classification of chest x-ray imagesusing cnn to detect pneumonia. 2020 10th International Conference On Cloud Computing, Data Science & Engineering (Confluence). pp. 227-231 (2020)
- [41] Stephen O., Sain M., Maduh U. &Jeong D. An efficient deep learning approach to pneumonia classification in healthcare. *Journal Of Healthcare Engineering*. 2019 (2019) <https://doi.org/10.1155/2019/4180949> PMID: 31049186
- [42] Zhang J., Xie Y., Pang G., Liao Z., Verjans J., Li W., et al. & Others Viral Pneumonia Screening onChest X-rays Using Confidence-Aware Anomaly Detection. *IEEE Transactions On Medical Imaging*.(2020)
- [43] Tuncer T., Ozyurt F., Dogan S. &Subasi A. A novel Covid-19 and pneumonia classification methodbased on F-transform. *ChemometricsAnd Intelligent Laboratory Systems*. 210 pp. 104256 (2021)<https://doi.org/10.1016/j.chemolab.2021.104256> PMID: 33531722
- [44] Jaiswal A., Tiwari P., Kumar S., Gupta D., Khanna A. & Rodrigues J. Identifying pneumonia in chest Xrays: A deep learning approach. *Measurement*. 145 pp. 511–518 (2019) <https://doi.org/10.1016/j.measurement.2019.05.076>